

## TID AND NIEL ASSESSMENT IN ALPHA IRRADIATED PHASE CHANGE MEMORY CELLS BASED ON SIMULATIONS

N. S. ZDJELAREVIĆ<sup>a,b\*</sup>, M. Lj. VUJISIĆ<sup>a</sup>

<sup>a</sup>*Faculty of Electrical Engineering, University of Belgrade, Belgrade, Serbia*

<sup>b</sup>*Public Company "Nuclear Facilities of Serbia", Vinča, Belgrade, Serbia*

Monte Carlo simulations of alpha irradiation on phase change memory cells were conducted and total ionizing dose and nonionizing energy loss in the whole cell was assessed. Phase change memory cell consists of bottom electrode, phase change layer and a top electrode. Bottom electrode has two different parts: top electrode cap made of high resistivity material and lower element made of low resistivity material. Materials used for phase change layers are chalcogenide alloys  $\text{Ge}_2\text{Sb}_2\text{Te}_5$ ,  $\text{Si}_2\text{Sb}_2\text{Te}_5$  and  $\text{Ag}_{3.5}\text{In}_{3.8}\text{Sb}_{7.5}\text{Te}_{17.7}$ . Changes induced in the investigated memory cells were presented.

(Received May 8, 2015; Accepted July 3, 2015)

*Keywords:* Phase change memory, Phase change materials, Alpha irradiation, Monte Carlo method, TID, NIEL

### 1. Introduction

Chalcogenide materials are vital materials used for storing information in phase change memories (PCM), which represent the most promising candidate for the next generation of non-volatile memory due to its high read/write speed, low power, high density, high retention and good compatibility with CMOS fabrication process. Electronic switching in amorphous chalcogenides, first observed in 1968. by Ovshinsky [1], lead to the first demonstration of phase change memory array in 1970 [2], but only after recent progress in the development of rapid crystallization alloys, could phase change alloys be used for practical high performance memory devices.

Every electronic device is continuously exposed to radiation both at space level and at sea level. Electronics devices at space levels are hit by ionizing particles originated from cosmic rays and the solar wind, while at ground level, ionizing particles (i.e. alpha particles) are generated by radioactive impurities in materials used in the chip package. Alpha particles emitted by traces of radioactive elements (thorium or uranium) that are present in the packaging materials of the device can penetrate in the memory device and corrupt the stored information [3].

Sensitivity of electronic devices to radiation has increased dramatically over the past decades due to constant reduction of their dimensions and operating voltages in order to satisfy consumer's growing demand for higher density, functionality, and lower power. Electronics reliability and dependability can be strongly influenced by radiation environment and radiation effects, therefore, radiation testing is becoming an important step in the manufacturing process. Before these costly and time consuming radiation test, which may include component irradiations at accelerating facilities, simulations of radiation effects and assessment of dose ranges in which these effects are expected should be conducted [4,5].

This paper presents the results of simulation-based assessment of Total Ionizing Dose (TID) and Nonionizing Energy Loss (NIEL) in alpha irradiated phase change memory cells for different phase change materials and different thicknesses and for different alpha energies and fluences.

---

\* Corresponding author: nena\_flo@hotmail.com

## 2. Operational principle and basic structure of a pcm cell

PCM operation relies on reversible phase transitions between the crystalline and amorphous state in some chalcogenide materials such as  $\text{Ge}_2\text{Sb}_2\text{Te}_5$  (GST),  $\text{Si}_2\text{Sb}_2\text{Te}_5$  (SST) and  $\text{Ag}_{3.5}\text{In}_{3.8}\text{Sb}_{7.5}\text{Te}_{17.7}$  (AIST). These two states exhibit different electrical resistivity which differs by several orders of magnitude, and PCM cell exploits this difference to store data. The programming of a PCM cell includes a RESET operation and a SET operation and is controlled by a current pulse (Figure 1). The RESET operation is based on phase transition from low resistivity, crystalline state (SET state) to higher resistivity, amorphous state (RESET state), whereas the SET operation is based on the reverse phase transition. To RESET a cell, a melt-quench effect is used: a very short and high current pulse is applied, which will induce enough Joule heating to first melt PCM partially as the temperature of the chalcogenide material raises above its melting point, and then upon the determination of the pulse, it quenches rapidly, leaving a region of amorphous material in a PCM cell. To SET the PCM cell, a rather long current pulse is applied to heat the material above its crystallization (glass transition) temperature, but below its melting temperature, during a time sufficiently long (typically in the order of 100 ns), so that all atoms can rearrange in their crystalline structure [6,7].

The basic structure of a PCM cell in a mushroom design, used for the simulations in our work is shown in Fig. 2.

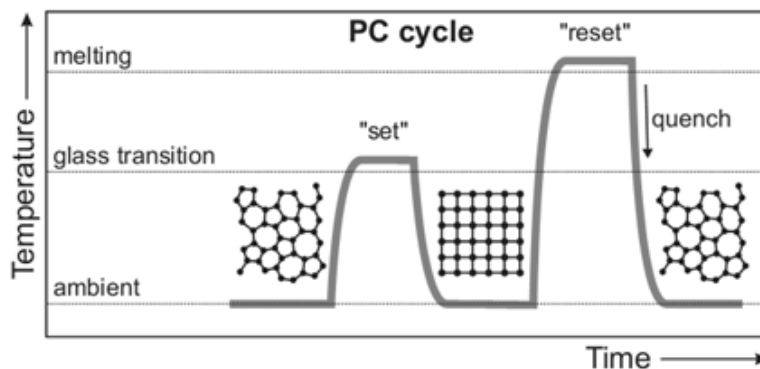


Fig. 1. Programming of a PCM cell [7]

Basically, a PCM cell is composed of a bottom electrode, named heater, surrounded by dielectric material, a thin chalcogenide film (phase change material) and a top electrode. The bottom electrode has two parts, a main element, and a top, upper portion, electrode cap. The electrode cap is formed of a high resistivity material, while main, lower, element is formed of a low resistivity material. The highly resistive electrode cap, which is close to the programmable volume of the chalcogenide material, creates a partial heating of the programmable volume by the resistive heating in the electrode cap. In embodiment, used for our simulations, the bottom electrode height was 100 nm, where main element was 80 nm high, and the electrode cap was 20 nm high. The high of upper electrode was 100 nm. The thickness of the phase change material was in the range of 25 nm to 125 nm. The low resistivity material used for the upper electrode and the lower part of the bottom electrode was TiW, and TaN was used for high resistivity cap [8].

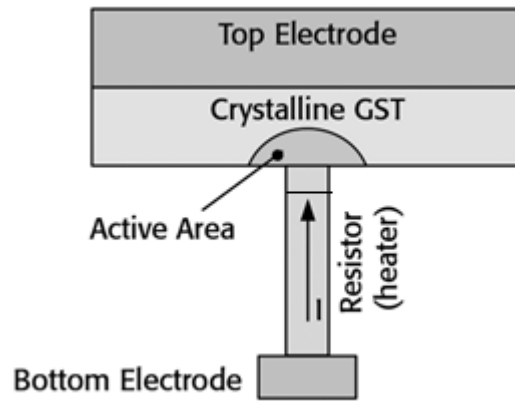


Fig. 2. Basic structure of a PCM cell

### 3. Radiation effects in pcm cells (nonionizing and ionizing energy losses )

When charged particle, i.e. alpha particle, traverses the matter, it interacts with its atoms and electrons and loses energy to both ionizing and nonionizing effects. Ionization energy loss refers to a process in which incoming particle interacts with electrons of the target atom resulting in electronic ionization or excitation of the atom. Most of the alpha energy is lost through ionization. The remaining portion of the alpha energy is lost through nonionizing events, where target atom is displaced. This displaced atom is commonly called the primary knock-on atom (PKA) and if its imparted energy is large enough, it can produce secondary displacements creating a cascade of displacements and potentially defect clusters. NIEL (Nonionizing Energy Loss) represents the rate at which energy is lost to these nonionizing events. It is a direct analog to stopping power for ionizing events.

NIEL values were obtained in this paper using the modified Kinchin-Pease relationship between the number of atomic displacements  $N_d$  and the nonionizing energy  $E_n$  and the rate of vacancy formation (obtained from Monte Carlo simulations), i.e.:

$$N_d = 0.8 \frac{E_n}{E_d},$$

where  $T_d$  is the threshold energy for atomic displacement (in eV). This equation is valid for  $E_n > 2.5 T_d$  [9].

Irradiated electronics can be sensitive to the ionizing and/or nonionizing dose deposited by the radiation and it has been found that radiation effects on the electrical parameters of the irradiated semiconductors display a simple, usually linear, relationship with NIEL. Therefore, in this paper we assessed the linear energy transfer (LET) ( i.e. total ionizing dose (TID)) and NIEL in the examined chalcogenide materials after conducting the simulations of alpha irradiation.

### 4. Monte Carlo simulation of alpha irradiation of pcm cell

Monte Carlo simulations of alpha particle transport through the PCM cell were performed in TRIM software, being part of the SRIM 2013 programming package. This TRIM code implements the so-called ZBL stopping, based on the model given by Ziegler, Biersack and Littmark. Simulations were restricted to monoenergetic unidirectional beams, incident perpendicularly on the surface of the PCM cell. The default values of threshold displacement energy for Ge, Sb, Te and Si atoms provided by SRIM were changed to the following values obtained by different studies: 20 eV for Ge [10], 9 eV for Sb [11], 7.8 eV for Te [12], 21 eV for

Si [10], 39 eV for Ag [13] and 7 eV for In [10]. Instead of calculated values for the densities of GST, AIST, and TiW offered by SRIM, more realistic values were used: 6.3 g/cm<sup>3</sup> for GST, 6.56 g/cm<sup>3</sup> for AIST, and 14.8 g/cm<sup>3</sup> for TiW [14]. Beam energy was varied across typical alpha energy ranges encountered in space and natural human environment (from 100 keV to 250 keV). For each alpha energy, particle transport simulations were run for all three phase change materials: GST, SST and AIST, varying the thickness of the phase change layer (from 25 nm to 125 nm). A *Detailed Calculation with Full Damage Cascades* was used as a type of TRIM calculations in order to obtain the most detailed files on alpha interactions with the PCM structure.

After conducting Monte Carlo simulations of transport of alpha particle through the PCM cell, output files, containing ion's ionization energy losses in the material, both due to ions and recoils, vacancy production rates for each target atom separately, as well as cell's dimensions and densities of the constituting materials, were used as input data for a MatLab code that calculated LET and NIEL along the depth of a phase change layer, and TID in the whole PCM cell.

## 5. Results of tid and niel calculations and discussion

The results of simulations and assessment of NIEL and TID in the alpha irradiated phase change memory cells are shown in figures 3, 4 and 5.

Figure 3 shows simulations and calculation results for PCM cell irradiated with 100 keV alpha particle (1000 particles) when the phase change material is GST. Figure 3(a) presents ionization energy losses in the materials of the PCM cell due to ions and recoils. It is obvious that energy losses due to ionization induced by ions are dominant compared to ionization induced by recoiled atoms. Figure 3(b) shows energy losses to the target producing Ge, Sb and Te vacancies. It is evident that incoming alpha particle mostly loses its energy on production of Te and Sb vacancies, and 2 or 3 times less energy on production of Ge vacancies. Mass energy losses (LET and NIEL) along the depth of a 100 nm GST film are shown in Fig. 3(c). Ionizing energy losses generally dominate NIEL losses by 2-3 orders of magnitude for the GST material when incoming particles are alpha particles.

On figure 3(d), TID in the whole PCM cell vs. alpha energy for thicknesses of the GST layer which are of interest is presented. By increasing alpha energy from 100 keV to 250 keV, TID value drops one order of magnitude (from the maximum value of  $9.6 \cdot 10^5$  Gy to the minimum value of  $3.9 \cdot 10^4$  Gy). Also, TID values increase with the increase of the thickness of the GST layer (i.e. thickness of the whole PCM cell).

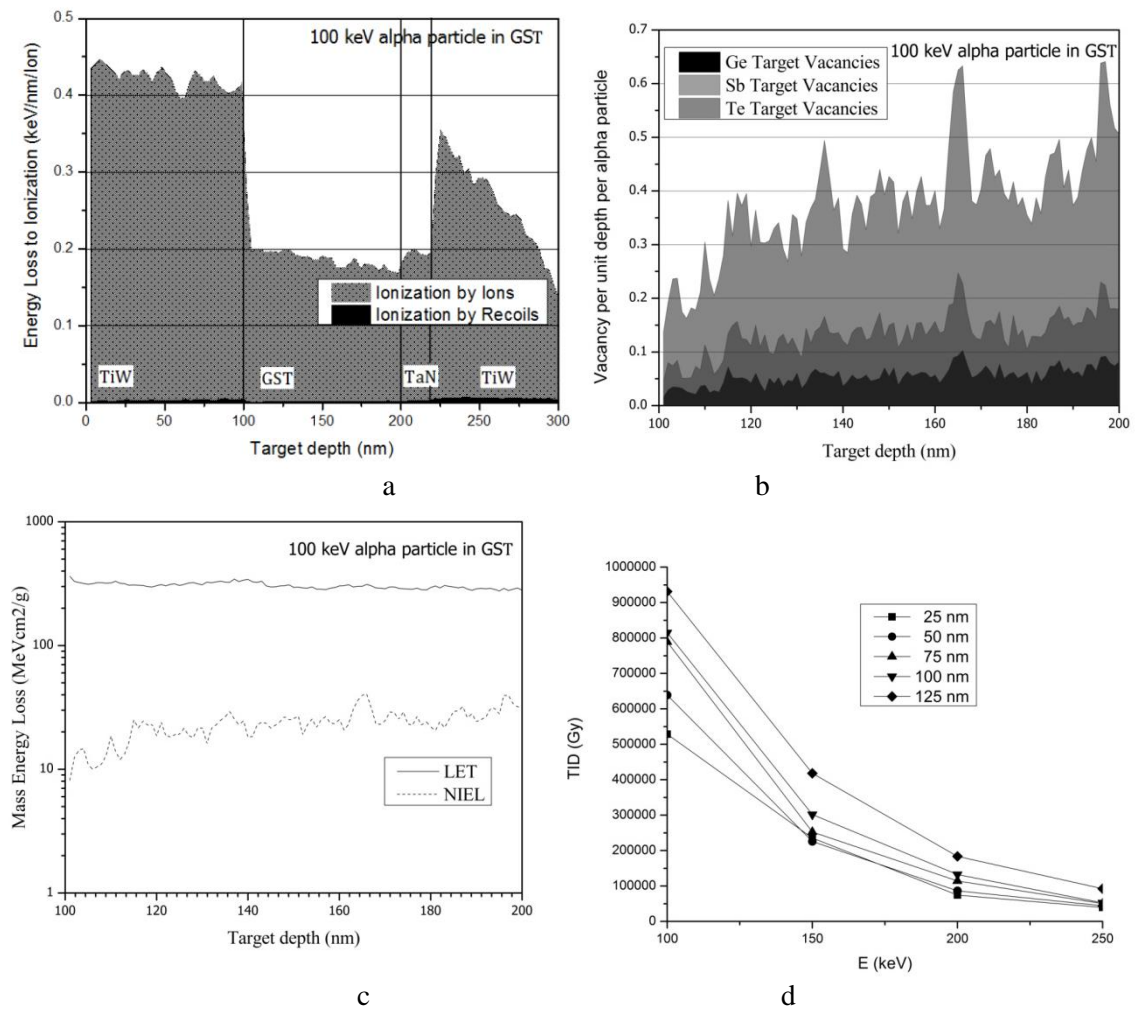


Fig. 3. Alpha particles (1000 histories) incident perpendicularly on the surface of the PCM cell when active material is GST (a) Ionization energy losses due to ions and recoils for 100 keV alpha particles, (b) Ge, Sb and Te target vacancies per unit depth and per alpha particle (100 keV), (c) Mass energy losses for 100 keV alpha particles, and (d) TID in the whole PCM cell vs. alpha energy for different thicknesses of the GST.

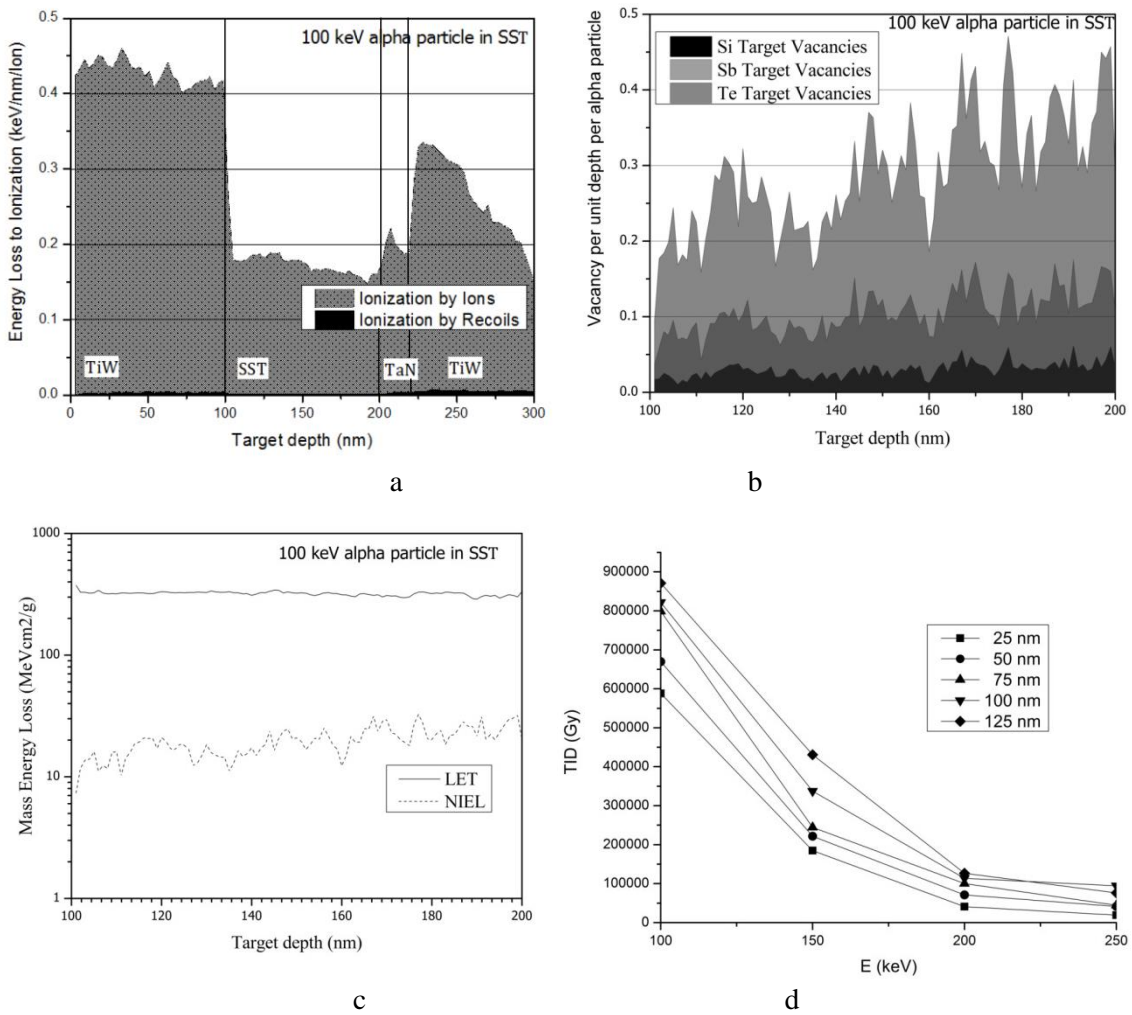


Fig. 4. Alpha particles (1000 histories) incident perpendicularly on the surface of the PCM cell when active material is SST (a) Ionization energy losses due to ions and recoils for 100 keV alpha particles, (b) Si, Sb and Te target vacancies per unit depth and per alpha particle (100 keV), (c) Mass energy losses for 100 keV alpha particles, and (d) TID in the whole PCM cell vs. thickness of the SST layer for different energies of alpha particles.

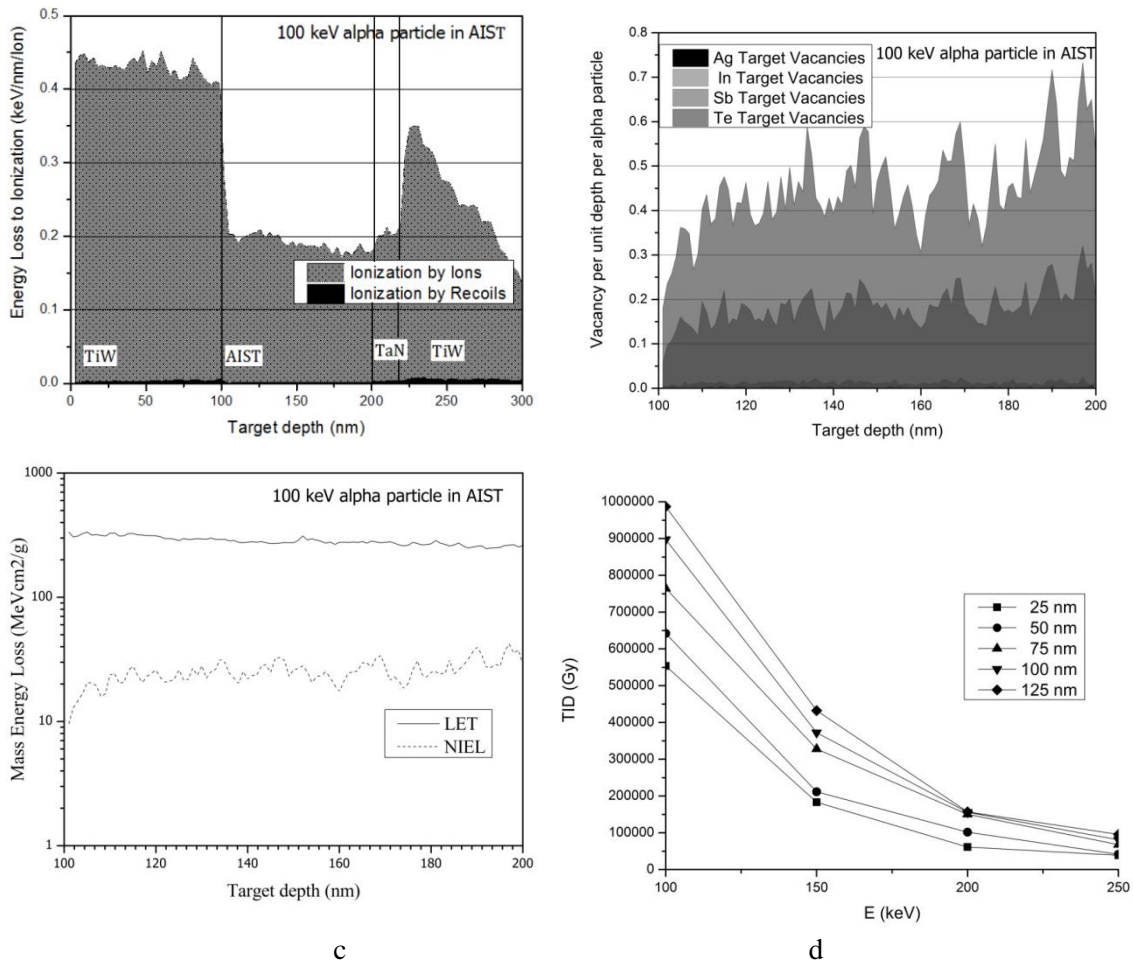


Fig. 5. Alpha particles (1000 histories) incident perpendicularly on the surface of the PCM cell when active material is AIST (a) Ionization energy losses due to ions and recoils for 100 keV alpha particles, (b) Ag, In, Sb and Te target vacancies per unit depth and per alpha particle (100 keV), (c) Mass energy losses for 100 keV alpha particles, and (d) TID in the whole PCM cell vs. alpha energy for different thicknesses of the AIST

Fig. 4 presents simulation results and calculations for PCM cell irradiated with 100 keV alpha particle (1000 particles) when SST is the phase change material. Figure 4(a) shows energy loss due to ionization in the PCM cell. Energy loss due to ionization induced by ions is larger than loss due to recoils. Figure 4(b) shows energy loss due to production of Si, Sb and Te vacancies in the target material. The least energy is lost for the production of Si vacancies, and the most for the production of Sb vacancies. In the Figure 4(c), LET and NIEL along 100nm of SST is shown. Nonionizing energy loss dominates by several orders of magnitude the ionizing energy loss. Figure 4(d) shows the assessed TID in whole PCM cell, with the SST layer vs. alpha energy for various thicknesses of the SST layer. If alpha energy is increased from 100 keV to 250 keV, TID drops one order of magnitude. Maximum value of TID in the PCM cell having SST layer is  $8.7 \cdot 10^5 \text{ Gy}$  and is slightly smaller than in the case of the PCM cell with GST layer, but of the same order of magnitude, the minimal value is  $1.9 \cdot 10^4 \text{ Gy}$  and is also smaller than in the case of the cell with the GST layer. TID increases with the increase of the SST thickness.

Figure 5 shows results of simulations and calculations in the case of 100 keV alpha particles (1000 particles) and PCM cell having AIST layer. Figure 4(a) shows energy loss of alpha particle due to ionization both by target ions and recoils. Like in the previous cases, loss due to ionization by ions is more significant than loss due to ionization by recoils. Figure 4(b) shows energy loss due to production of Ag, In, Sb and Te vacancies. The most energy of the alpha particle is lost due to production of Sb and Te vacancies, while less energy is lost due to

production of Ag and In vacancies. Ionizing and nonionizing energy losses along the depth of a 100 nm AIST layer are shown in Figure 4(c). For alpha particles of given energy, LET dominates NIEL in the specified AIST layer. Figure 4(d) presents calculated values of TID in the whole PCM cell with AIST layer for different alpha energies and for different AIST thicknesses. Maximal value of TID ( $9.9 \cdot 10^5 \text{Gy}$ ) is obtained for 100 keV alpha and 125 nm AIST, while minimal value ( $3.8 \cdot 10^4 \text{Gy}$ ) is obtained for 250 keV alpha and 25 nm AIST.

## 6. Conclusion

Monte Carlo simulations of alpha interactions with PCM cell having different phase change materials were conducted. Ionizing and nonionizing energy losses were assessed and analyzed. Analysis of ionization energy losses due to ions and recoils in PCM cell having GST, SST and AIST as an active layer showed that energy loss due to ions is dominant compared to ionization induced by recoiled atoms for all three materials. Energy loss due to vacancy production is greatest for Sb and Te vacancies, and smallest for Ag, In, Si and Ge, respectively. Generally, ionizing energy losses dominate nonionizing losses by 2-3 orders of magnitude. TID value drops one order of magnitude with increase of alpha energy from 100 keV to 250 keV. TID values are slightly different for these three materials, AIST having the largest TID, followed by GST and SST.

## References

- [1] S. Ovshinsky, *Physical Rev. Lett* **21**, 1450 (1968).
- [1] R.G. Neale, D.L. Nelson, G.E. Moore, *Electronics* **43**, 56 (1970).
- [3] K. SangBum, PhD dissertation of Departement of Electrical Engineering, Stanford University, 12 (2010).
- [4] M. Vujisic, K. Stankovic, E. Dolicanin, P. Osmokrovic, *Radiation Effects and Defects in Solids: Incorporating Plasma Science and Plasma Technology* **165**, 362 (2010).
- [5] N.Zdjelarevic, I. Knezevic, M. Vujisic, LJ. Timotijevic, *Nucl. Technol. Radiat.* **28**, 299 (2013).
- [6] H.S.P Wong, S.Raoux, S. Kim, J. Liang, J.P.Reifenberg, B. Rajendran, M. Asheghi, K.E. Goodson, *Proceedings of the IEEE* **98**, 2201 (2010).
- [7] P. Zalden, Doctoral Dissertation in Science, Rheinisch-Westfaelischen Technischen Hochschule Aachen, (2012).
- [8] J. Liu, United States Patent 7,684,235 B2, (2010).
- [9] S.R. Messenger, E.A. Bruke, G.P. Summers, M.A. Xapsos, R.J. Walters, E.M. Jackson, B.D. Weaver, *IEEE Transactions on Nuclear Science* **46**, 1595 (1999).
- [10] I. Jun, M.A. Xapsos, E.A. Burke, *IEEE Transactions on Nuclear Science* **51**, 3207 (2004).
- [11] F.H. Eisen, *Physical Review* **135**, A1394 (1964).
- [12] F.J. Bryant, A.F.J. Cox, E. Webster, *J. Physics C: Solid State Physics* **1**, 1737 (1968).
- [13] G.H.M. Broeders, A.Yu. Konobeyev, *Forschungszentrum Karlsruhe FZKA 7197*, 8 (2006).
- [14] L.W. Qu, X.S. Miao, J.J. Sheng, Z. Li, J.J. Sun, P. An, J.H.D. Yang, C. Liu, *Solid-State Electronics* **56**, 191 (2011).